

# Periodic trajectories in the regular pentagon

Diana Davis,<sup>\*</sup> Dmitry Fuchs,<sup>†</sup> and Serge Tabachnikov<sup>‡</sup>

February 4, 2011

To the memory of V. I. Arnold

## 1 Introduction

The study of billiards in rational polygons and of directional flows on flat surfaces is a fast-growing and fascinating area of research. A classical construction reduces the billiard system in a rational polygon – a polygon whose angles are  $\pi$ -rational – to a constant flow on a flat surface with conical singularities, determined by the billiard polygon. In the most elementary case, the billiard table is a square and the surface is a flat torus obtained from four copies of the square by identifying pairs of parallel sides. We refer to [4, 6, 9, 12, 15, 16] for surveys of rational polygonal billiards and flat surfaces.

It is well known that the dynamics of a constant flow on a flat torus depends on the direction: if the slope is rational then all the orbits are closed; and if the slope is irrational then all the orbits are uniformly distributed. The same dichotomy holds for the billiard flow in a square. This property is easy to deduce from the fact that a square tiles the plane by reflections in its sides. In the seminal papers [13, 14], W. Veech discovered a large class of

---

<sup>\*</sup>Department of Mathematics, Brown University, Providence, RI 02912, USA; e-mail: [diana@math.brown.edu](mailto:diana@math.brown.edu)

<sup>†</sup>Department of Mathematics, University of California, Davis, CA 95616, USA; e-mail: [fuchs@math.ucdavis.edu](mailto:fuchs@math.ucdavis.edu)

<sup>‡</sup>Department of Mathematics, Pennsylvania State University, University Park, PA 16802, USA; e-mail: [tabachni@math.psu.edu](mailto:tabachni@math.psu.edu)

polygons and flat surfaces that satisfy the same dynamical dichotomy as the square (it is now called the Veech dichotomy or the Veech alternative). This class includes the isosceles triangle with the angles  $(\pi/5, \pi/5, 3\pi/5)$  and the regular pentagon; neither tiles the plane by reflection.

This paper is devoted to a case study of these two polygonal billiards, namely, to a detailed description of periodic billiard trajectories. The flat surface corresponding to the  $(\pi/5, \pi/5, 3\pi/5)$ -triangle is the *double pentagon*, an oriented surface of genus 2 constructed from two centrally symmetric copies of the regular pentagon by identifying pairs of parallel sides by parallel translation. The transition between billiards and flat surfaces is shown in Figure 1. First, we take 10 copies of the triangle and tile with them a star-like decagon; a billiard trajectory in the triangle (Figure 1 (a)) becomes a sequence of parallel intervals in the decagon (Figure 1 (b)) which, in turn, becomes a geodesic on a flat surface of genus 2 obtained from the decagon by attaching parallel sides by means of parallel translation. We rearrange this decagon into a double pentagon by cutting off five triangles by dashed lines and then parallel translations of these triangles so that they form a second (bottom) pentagon (Figure 1 (c)). The last step shown in Figure 1 (d) is a transition to a billiard trajectory in a regular pentagon. The latter is also equivalent to the directional flow on a flat surface; this surface is glued together from ten copies of the regular pentagon and has genus 6. The latter surface admits a 5-fold covering of the former one (see [14]), so a linear periodic trajectory in the double pentagon gives rise to a periodic billiard trajectory in the regular pentagon; the period of the latter may be the same or five times that of the one on the double pentagon; see Section 2.6.

A periodic billiard trajectory in a polygonal billiard is always included into a 1-parameter family of periodic trajectories. If the period is even, one has a strip of parallel trajectories having the same length and the same combinatorial period; if the period is odd, nearby parallel trajectories have the length and the period twice as large. When talking about periodic billiards orbits, we always mean even-periodic ones, and always consider a family of parallel orbits.

Our motivation in this study is two-fold. First, it is an intriguing problem to describe closed geodesics on the surfaces of regular polyhedra in 3-space, in particular, of a regular dodecahedron [2, 3]. The classifications of closed geodesics on a regular dodecahedron and closed billiard trajectories in a regular pentagon are closely related; we do not consider the dodecahedron problem here, but we hope to return to it in the near future. Secondly, we

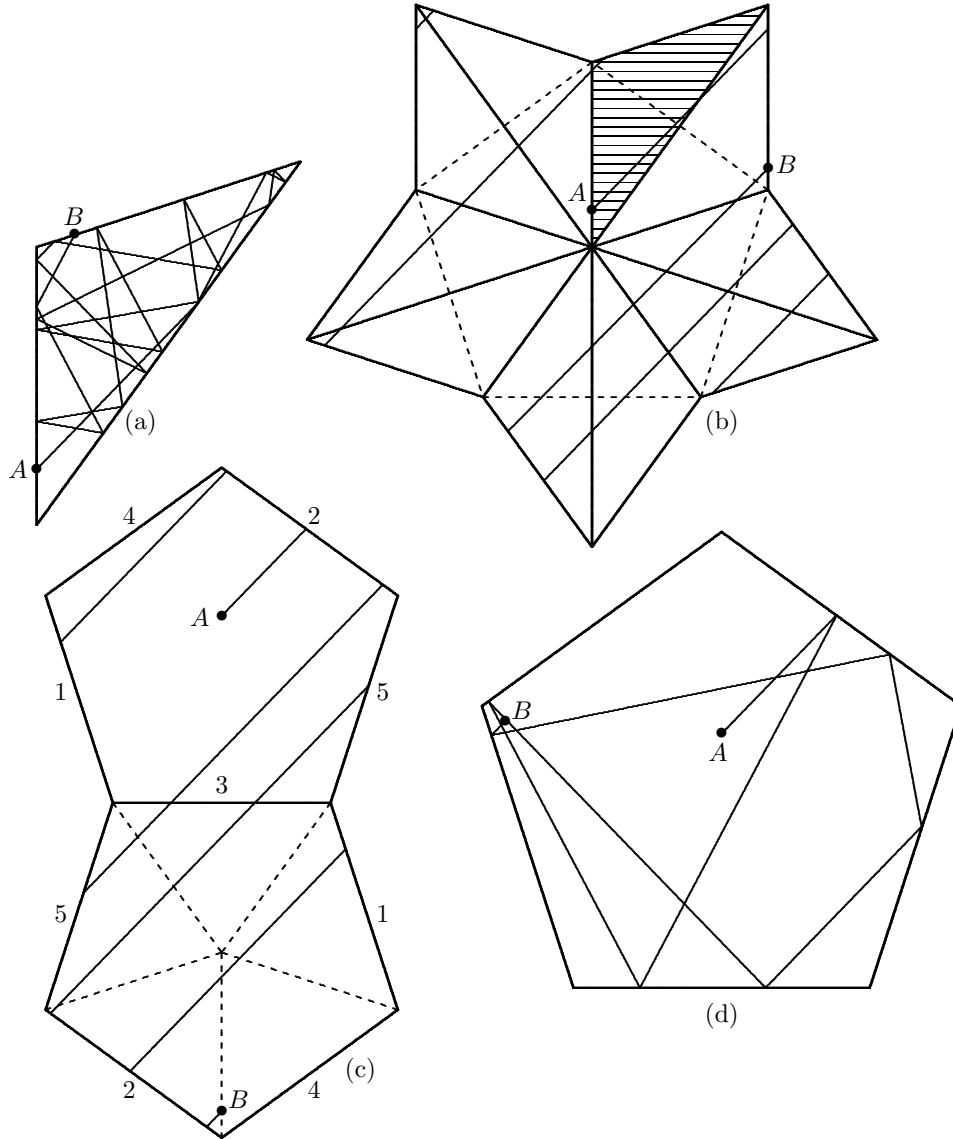


Figure 1: (a)  $(\pi/5, \pi/5, 3\pi/5)$ -triangle with a billiard trajectory; (b) a star-like decagon with the same trajectory; (c) a double pentagon with the same trajectory; (d) a regular pentagon with the same billiard trajectory.

were inspired by a recent study by J. Smillie and C. Ulcigrai of the linear trajectories on the flat surface obtained from a regular octagon by identifying the opposite sides [10, 11]. We obtain a number of results for the double pentagon that are analogous to the results in [10, 11], but we also go further: some of our results are new in the case of the octagon as well.

It is well known that constant flows on flat surfaces are intimately related with interval exchange transformations: one obtains an interval exchange as a 1-dimensional section of a constant flow and the first return map to this section. In our situation, we have the following equivalent description of the constant flows on the double pentagon depicted in Figure 2.

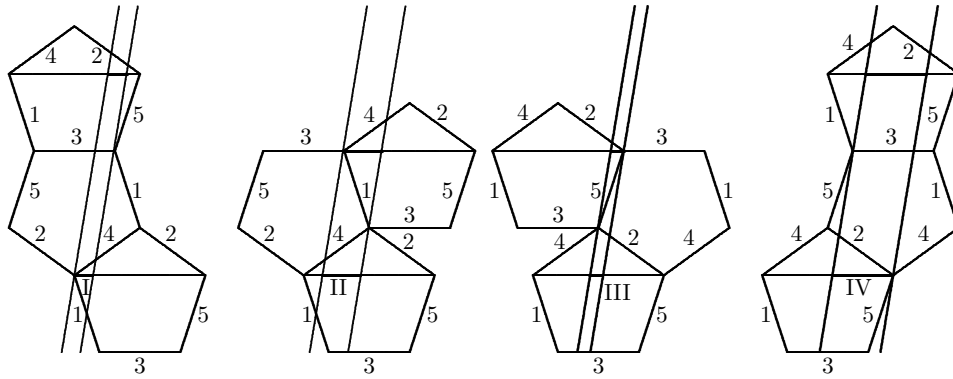


Figure 2: Reduction to an interval exchange map

Choose a diagonal of the pentagon as a section of a constant flow on the double pentagon and assume that the angle between the trajectory and the diagonal is between  $72^\circ$  and  $90^\circ$ . An exchange of four intervals arises, permuted as follows:  $\begin{pmatrix} \text{I} & \text{II} & \text{III} & \text{IV} \\ \text{III} & \text{I} & \text{IV} & \text{II} \end{pmatrix}$ , see Figure 3.

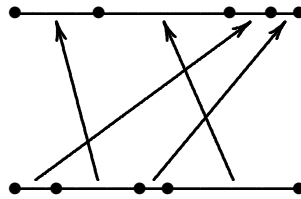


Figure 3: Interval exchange map

If the length of the side of the pentagon is 1, then the length of the

diagonal is the golden ratio  $\phi = \frac{1 + \sqrt{5}}{2}$ , and if we consider the domain of our map as the interval  $[0, \phi]$ , then the division points are

$$\frac{1}{2} - u(\phi + 1), \frac{\phi}{2} - u, -\frac{1}{2} - u(\phi - 1) + \phi.$$

Here  $u = \frac{\sin 36^\circ}{\lambda}$  where  $\lambda$  is the slope of the trajectory. Our condition on the angle takes the form  $0 \leq u \leq 1 - \phi/2 \approx 0.19$ .

We shall use both descriptions, directional flows on the double pentagon and the interval exchange map, interchangeably.

**Acknowledgments.** D.F. and S.T. are grateful to the Mathematisches Forschungsinstitut Oberwolfach whose hospitality they enjoyed during their Research in Pairs stay in summer of 2010. D.F. is grateful to IHES for an inspiring atmosphere and excellent working conditions during his visit in summer of 2010. We are grateful to J. Smillie and A. Zorich for interesting discussions, and to R. Schwartz for the graduate topics course on piecewise isometries that he taught in spring of 2010.

## 2 Statements of results

### 2.1 Directions

We start with a remark that the double pentagon has an involution, the central symmetry that exchanges the two copies of the regular pentagon. This involution interchanges linear trajectories having the opposite directions. For this reason, when talking about the direction of a trajectory, we do not make a distinction between the directions  $\alpha$  and  $\alpha + \pi$ . In other words, the set of directions is the real projective line  $\mathbb{RP}^1$ .

We identify  $\mathbb{RP}^1$  with the circle at infinity (absolute) of the hyperbolic plane in the Poincaré model. The five directions of the diagonals of the pentagon are periodic: the double pentagon decomposes into two strips of parallel periodic trajectories, see Figure 4.

The directions of the diagonals of the pentagon form the vertices of an ideal regular pentagon in the hyperbolic plane.<sup>1</sup> We call this ideal pentagon

---

<sup>1</sup>An ideal polygon is regular if the cross-ratio of each consecutive quadruple of its vertices is the same.

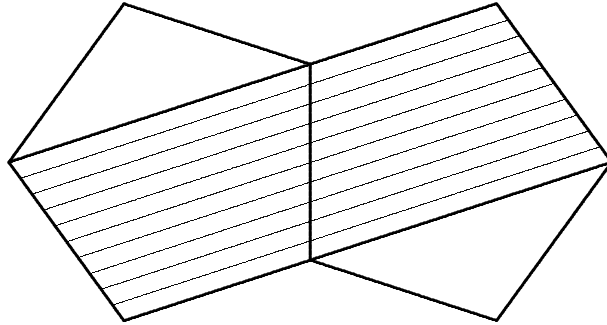


Figure 4: Two strips covering the double pentagon: a shadowed wider and longer strip and a white narrower and shorter strip

the pentagon of 0th generation. The five arcs of  $\mathbb{RP}^1$  bounded by the vertices of this ideal pentagon correspond to the five cones of directions in Figure 5. We consider the 3rd sector as a principal one and focus on periodic directions in this sector.

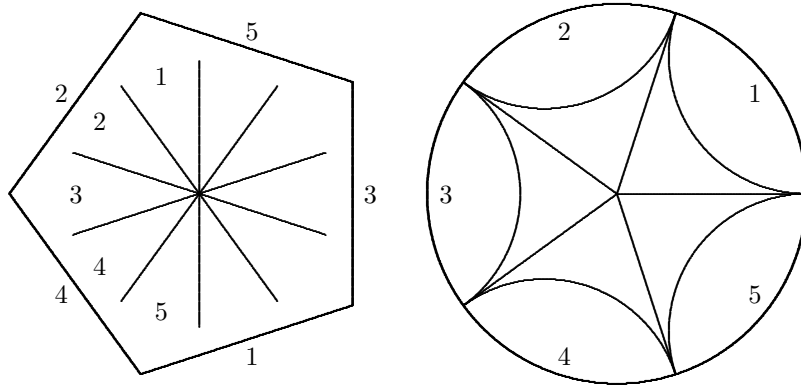


Figure 5: Sectors of directions on the absolute

We choose an affine coordinate on  $\mathbb{RP}^1 = \mathbb{R} \cup \infty$  in such a way that the vertices of the ideal regular pentagon of 0th generation have the coordinates  $1 - \frac{\phi}{2}, \frac{\phi}{2}, \infty, -\frac{\phi}{2}, \frac{\phi}{2} - 1$  where  $\phi = \frac{1 + \sqrt{5}}{2}$  is the Golden Ratio (this choice is unique, up to a fractional-linear transformation).

Let  $\Gamma$  be the group of isometries of the hyperbolic plane generated by the clockwise rotation  $T$  by  $72^\circ$  and the reflection  $R$  in the vertical side of the pentagon of 0th generation; these transformations act on  $\mathbb{RP}^1$  by the

formulas

$$T(x) = \frac{2\phi x + 3 - \phi}{2\phi - 4x}, \quad R(x) = \frac{1}{4\phi^4 x}.$$

The action of  $\Gamma$  creates smaller pentagons of the 1st, 2nd, etc., generations, see Figure 6. We are interested in points to the left of the geodesic  $\left(1 - \frac{\phi}{2}, \frac{\phi}{2} - 1\right)$ ; on this arc of the absolute the vertices of the pentagon of  $k$ th generation are denoted by  $\alpha$  with  $k$  indices as shown in Figure 6. For example, the pentagon bounded by the arc  $(\alpha, \alpha_1)$  has vertices  $\alpha, \alpha_{01}, \alpha_{02}, \alpha_{03}, \alpha_1$ , and the pentagon bounded by the arc  $(\alpha_{011}, \alpha_{012})$  has vertices  $\alpha_{011}, \alpha_{0111}, \alpha_{0112}, \alpha_{0113}, \alpha_{012}$ .

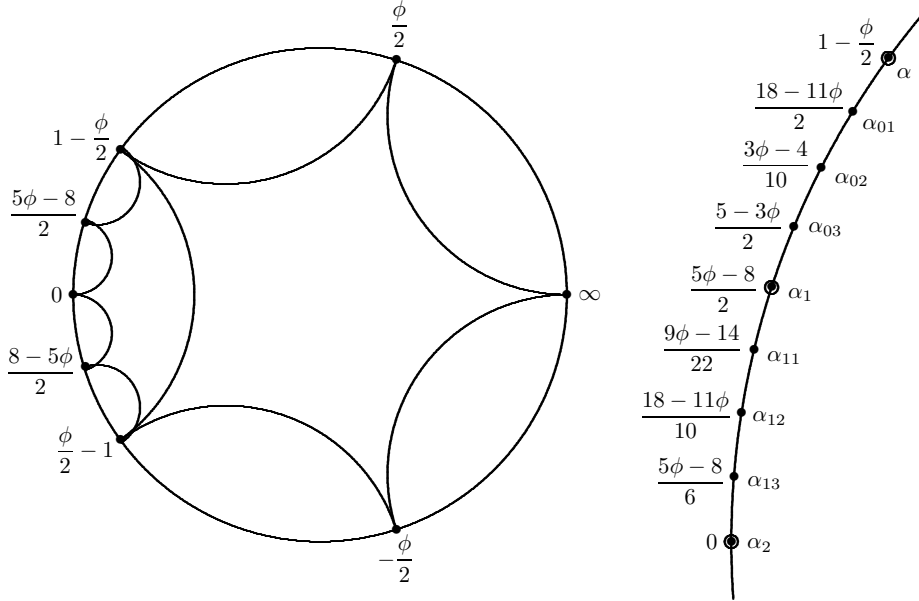


Figure 6: Directions of periodic geodesics

The next result (which is not genuinely new) summarizes information about periodic directions.

**Theorem 1** (i) *The set of directions of periodic trajectories (within the 3rd sector) is the set of numbers  $\alpha_{n_1 n_2 \dots n_k}$  with  $0 \leq n_i \leq 3$  and  $n_k \neq 0$ ;*  
(ii) *for each of these periodic directions, the double pentagon decomposes into the union of two strips of parallel periodic trajectories (see Figure 7);*

(iii) one has:

$$\alpha_{n_1 n_2 \dots n_k} = RT^{m_1} RT^{m_2} \dots RT^{m_k} \alpha$$

where

$$m_i = \begin{cases} 4 - n_i, & \text{if } i \text{ is even,} \\ n_i + 1, & \text{if } i \text{ is odd and } i \neq k, \\ n_i, & \text{if } i \text{ is odd and } i = k; \end{cases}$$

(iv) the set of periodic directions is  $\mathbb{Q}[\phi] \cup \{\infty\}$ .

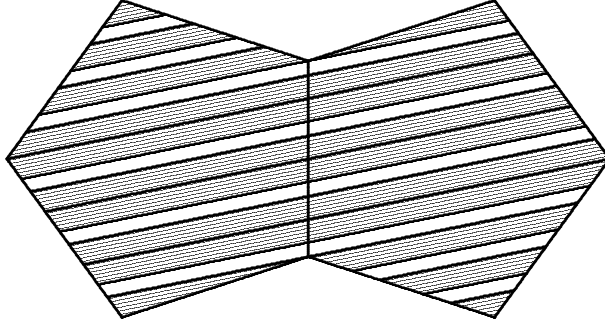


Figure 7: Two strips of regular periodic trajectories

**Remark 2.1** We note that

$$T^m(x) = -\frac{\phi}{2} - \frac{1}{-\phi - \frac{1}{\dots - \phi - \frac{1}{-\frac{\phi}{2} + x}}}$$

and this allows to transform the formula for  $\alpha_{n_1 n_2 \dots n_k}$  into a continued fraction in the spirit of [8].

## 2.2 Periods

We describe periodic trajectories symbolically in two ways. When dealing with the double pentagon, we label the sides by symbols 1, 2, 3, 4, 5, see Figure

5. Then a periodic linear trajectory has a symbolic orbit, a periodic word in these five symbols, consisting of the labels of the consecutively crossed sides. The (combinatorial) period of the trajectory is the period of this word. When we deal with the interval exchange model, we label the consecutive four intervals by symbols I, II, III, IV, and then a periodic trajectory has a symbolic orbit, a periodic word in these four symbols, consisting of the labels of the visited intervals.

The two codings translate into each as follows.

**Lemma 2.2** *The two forms of symbolic orbits correspond to each other according to the rule*

$$\{43\} \leftrightarrow \{I\}; \{41\} \leftrightarrow \{II\}; \{25\} \leftrightarrow \{III\}; \{23\} \leftrightarrow \{IV\}.$$

**Proof.** (See Figure 2.) We follow upward from the interval I, II, III, IV between the parallel lines and record the labels of the sides we cross.  $\square$

In particular, the period in the Roman numerals is half of the respective period in the Arabic ones.

The next theorem holds for both kinds of periods, “Roman” and “Arabic”. According to Theorem 1, to every periodic direction, represented by a point on arc of the absolute, there correspond two periods; we denote them by a pair of script and capital letters, such as  $a$  and  $A$ ,  $a \leq A$ .

**Theorem 2** *Let  $a, A$  and  $b, B$  be the pairs of periods for two points joined by a side of an ideal pentagon of some generation. Then, for the three additional vertices of the pentagon of the next generations, the periods are as shown in the diagram below:*

$$\begin{array}{r} a, A \\ b + A, a + A + B \\ A + B, a + b + A + B \\ a + B, b + A + B \\ b, B \end{array} \left. \vphantom{\begin{array}{r} a, A \\ b + A, a + A + B \\ A + B, a + b + A + B \\ a + B, b + A + B \\ b, B \end{array}} \right\}$$

The (Roman) periods for the points  $\pm(1 - \phi/2)$  are all equal to 1. Thus, we can compute the periods of all periodic orbits. For example, for the points shown in Figure 6, the periods are given in the following table.

Direction	Periods	Direction	Periods
$\alpha$	1,1	$\alpha_{11}$	5,9
$\alpha_{01}$	3,5	$\alpha_{12}$	7,11
$\alpha_{02}$	4,7	$\alpha_{13}$	6,9
$\alpha_{03}$	4,6	$\alpha_2$	2,4
$\alpha_1$	2,3		

When proceeding to further generations, the periods grow rapidly. For example, for the direction  $\alpha_{123123123}$  the two periods are 3932, 6334.

There exists an equivalent statement of Theorem 2.

**Theorem 3** *Let  $\beta$  be some of the directions  $\alpha_{n_1\dots n_k}$ , and let  $\dots, \gamma_{-2}, \gamma_{-1}, \gamma_0, \gamma_1, \gamma_2, \dots$  be all points connected by arcs (sides of ideal pentagons) with  $\beta$  and ordered as shown in Figure 8. Let  $(b, B)$  be the periods corresponding to the direction  $\beta$ , and let  $(c_i, C_i)$  be the periods corresponding to  $\gamma_i$  multiplied by  $-1$ , if  $i < 0$ . Then*

$$\dots, (c_{-2}, C_{-2}), (c_{-1}, C_{-1}), (c_0, C_0), (c_1, C_1), (c_2, C_2), \dots$$

*is an arithmetic sequence with the difference  $(B, b + B)$ .*

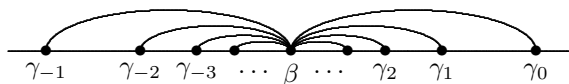
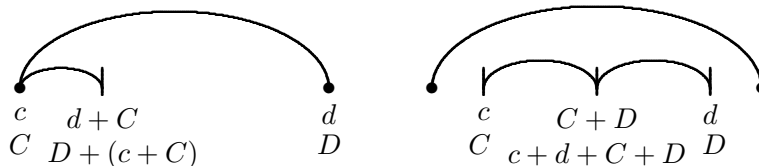


Figure 8: Periodic directions connected with a given periodic direction

**Proof.** We need to check that for any three vertices in a row of an ideal pentagon of any generation, the pairs of periods are as shown in the diagrams below (with some  $c, d, C, D$ )



(the left diagram may be reflected in a vertical line; in the right diagram, one of the ends of the upper arc may coincide with one of the three points with periods marked). To do this, it is sufficient to compare these diagrams with corresponding fragments of the diagram in Theorem 2.  $\square$

One may present the information on the periods in a different format. Encode the pair of (Roman) periods  $(a, A)$  by a single number  $a + \phi A \in \mathbb{Z}[\phi]$ . For example, such a period for the points  $\pm(1 - \phi/2)$  is  $1 + \phi = \phi^2$ . In this notation, Theorem 2 asserts that if  $U, V \in \mathbb{Z}[\phi]$  are the periods at two consecutive points of  $k$ th generation (from top to bottom, in Figure 6) then the respective periods in the  $(k + 1)$ st generation are

$$U, V + \phi U, \phi U + \phi V, U + \phi V, V.$$

This can be restated as follows: the consecutive pair  $(U, V)$  is replaced by four consecutive pairs

$$(U, V + \phi U), (V + \phi U, \phi U + \phi V), (\phi U + \phi V, U + \phi V), (U + \phi V, V)$$

obtained from the column vector  $(U, V)^T$  by the action of following matrices:

$$X_0 = \begin{pmatrix} 1 & 0 \\ \phi & 1 \end{pmatrix}, X_1 = \begin{pmatrix} \phi & 1 \\ \phi & \phi \end{pmatrix}, X_2 = \begin{pmatrix} \phi & \phi \\ 1 & \phi \end{pmatrix}, X_3 = \begin{pmatrix} 1 & \phi \\ 0 & 1 \end{pmatrix}.$$

One obtains the following consequence of Theorem 2.

**Theorem 4** *Given a periodic direction  $\alpha_{n_1 n_2 \dots n_k}$ , the respective period in  $\mathbb{Z}[\phi]$  is the first component of the vector*

$$X_{n_k} X_{n_{k-1}} \dots X_{n_1} \begin{pmatrix} \phi^2 \\ \phi^2 \end{pmatrix}.$$

### 2.3 Symbolic orbits

For every  $\alpha_{n_1 n_2 \dots n_k}$  ( $k \geq 0$ ,  $0 \leq n_i \leq 3$ ,  $n_k \neq 0$ ,  $k$  is the number of generation) there are two periodic symbolic orbits, defined up to a cyclic permutation: a “short” one and a “long” one (although for  $k = 0$  they have the same length). Below, we describe an algorithm which creates orbits for the  $(k+1)$ st generation from the orbits of  $k$ th generation. In this construction we use symbolic orbits arising from the double pentagon, i.e., the symbols used are 1, 2, 3, 4, 5. The construction is based on the graph depicted in Figure 9.



sandwiched symbols and deleting all other ones. For example, the reduction of the periodic word 5 2 3 4 3 2 3 4 3 2 is the periodic word 4 2 4 5.

The next result is converse to Theorem 5. A similar sandwiching property for octagons was discovered in [10].

**Theorem 6** *Consider a symbolic orbit, short or long, corresponding to a periodic direction  $\alpha_{n_1 n_2 \dots n_k}$ . Reduce this symbolic orbit and shift the reduced word (cyclically) by  $4 - n_1$ . The resulting cyclic word is the symbolic orbit corresponding to the periodic direction  $\alpha_{3-n_2, \dots, 3-n_{k-1}, 4-n_k}$ , short or long, respectively.*

To translate the symbolic orbits in the double pentagon into the language of the interval exchange map, we need to make the “inverse change”  $\{43\} \rightarrow \text{I}$ ,  $\{41\} \rightarrow \text{II}$ ,  $\{25\} \rightarrow \text{III}$ ,  $\{23\} \rightarrow \text{IV}$ .

**Lemma 2.3** *Every cyclic symbolic orbit in symbols  $\{1, 2, 3, 4, 5\}$  can be written as a cyclic word in symbols  $\{\text{I}, \text{II}, \text{III}, \text{IV}\}$ .*

**Proof.** The pairs in question are precisely the edges of the graph in Figure 9 oriented downward. A path in this graph has upward and downward edges alternating, hence the sequence of vertices passed can be split into pairs corresponding to downward edges.  $\square$

Assign to a “Roman” cyclic symbolic orbit the 4-vector whose components are equal to the number of symbols I, II, III, IV in the orbit. We denote the vectors corresponding to the short and the long orbits in the same direction by  $(c, d, e, f)$  and  $(C, D, E, F)$ .

**Theorem 7** *One has:  $C = c + e$ ,  $D = f$ ,  $E = c$ ,  $F = d + f$ .*

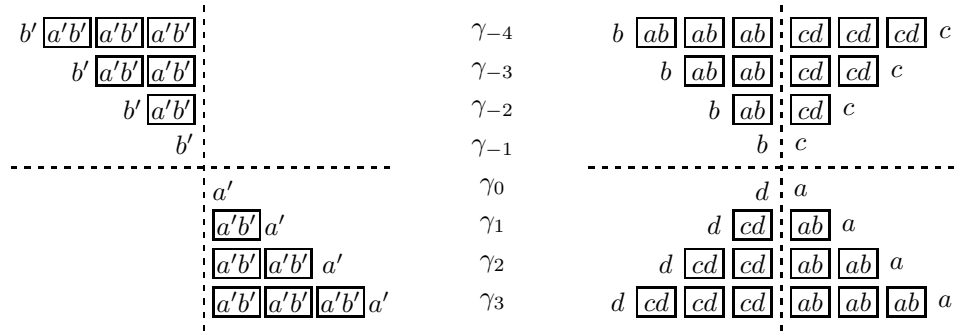
## 2.4 Further experimental results

We state below two more propositions concerning symbolic orbits. They are confirmed by a huge experimental material, and we hope to give their proofs in forthcoming publications. They can be regarded as symbolic counterparts of Theorems 2 and 3.

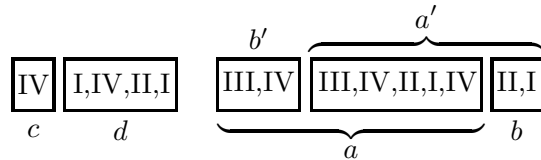
**Conjecture 8** Let  $a, A$  and  $b, B$  be two pairs of cyclic symbolic orbits corresponding to two periodic directions joined by a side of an ideal pentagon of some generation. Then one can cut the cyclic words  $a, A, b, B$  into linear ones, concatenate them, and close the words up to cyclic words, so that the cyclic symbolic orbits for the three additional vertices of the pentagon of the next generations (listed in the direction from the first point to the second) are:

$$\begin{aligned} bA, & \quad BaA; \\ AB, & \quad bBaA; \\ aB, & \quad AbB. \end{aligned}$$

**Conjecture 9** Let  $\beta$  and  $\dots, \gamma_{-2}, \gamma_{-1}, \gamma_0, \gamma_1, \gamma_2, \dots$  denote the same as in Theorem 3. Then there exist a splitting of the short symbolic orbit corresponding to  $\beta$  into two parts,  $(c, d)$ , and two splittings of the long symbolic orbit corresponding to  $\beta$  into two parts:  $(a, b) = (a', b')$  such that  $a$  and  $b'$  have the same beginning and such that the short and long symbolic orbits corresponding to  $\gamma_i$  look as shown in the diagram below



For example, the symbolic orbits for  $\beta = \alpha_{11}$  (in the exchange interval version) are IV, I, IV, II, I and III, IV, III, IV, II, I, IV, II, I. Their splittings from Theorem 9 are



Then  $\gamma_1 = \alpha_{111}$  and the symbolic orbits are

$$\underbrace{\text{III, IV, II, I, IV, II, I}}_{a'} \underbrace{\text{III, IV}}_{b'} \underbrace{\text{III, IV, II, I, IV, II, I}}_{a'}$$

and

$$\underbrace{\text{I, IV, II, I}}_d \underbrace{\text{IV, I}}_c \underbrace{\text{IV, II, I}}_d \underbrace{\text{III, IV, III, IV, II, I, IV, II, I}}_a \underbrace{\text{III, IV, III, IV, II, I, IV}}_b \underbrace{\text{III, IV, III, IV, II, I, IV}}_a$$

## 2.5 Lengths and displacement vectors

A linear trajectory on a flat surface unfolds to a straight line in the plane; a periodic linear orbit develops to a vector that we call the *displacement vector* of the periodic orbit. The displacement vector contains information about the direction and the length of the periodic orbit.

Let the vectors  $(c, d, e, f)$  and  $(C, D, E, F)$  have the same meaning as before.

**Theorem 10** *The displacement vectors of the short and the long periodic orbits are*

$$(c\phi + e)u + (f\phi + d)v \quad \text{and} \quad (C\phi + E)u + (F\phi + D)v$$

where  $u$  and  $v$  are the two diagonals bounding the 3rd sector, see Figure 10. The length of the respective short periodic orbit equals

$$m[(c + f)\phi + (d + e)], \quad m = \frac{\phi^2 \sin 36^\circ}{\cos \alpha}$$

where  $\alpha$  is the angle between the trajectory and the bisector of the vectors  $u$  and  $v$ ; the respective long periodic orbit is  $\phi$  times as long.

## 2.6 Periodic billiard orbits in the regular pentagon

We can relate closed billiard trajectories in the regular pentagon with linear periodic trajectories in the double pentagon.

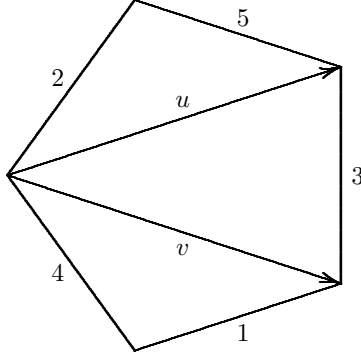


Figure 10: Vectors  $u$  and  $v$

**Theorem 11** *Let  $L$  be the length of closed trajectory of the double pentagon and  $(c, d, e, f)$  be the respective 4-component vector. Then the billiard trajectory in the regular pentagon, starting from the same point in the same direction is also periodic and its length is*

$$\begin{cases} L, & \text{if } (c - f) + 2(e - d) \equiv 0 \pmod{5} \\ 5L, & \text{if } (c - f) + 2(e - d) \not\equiv 0 \pmod{5} \end{cases}$$

**Proof.** Consider the left diagram in Figure 2. If we denote the vertices of the bottom pentagon as  $A, B, C, D, E$  and then make reflections in the side  $BC$  of this pentagon and in the side  $AE$  of the reflected pentagon, we will see that the pentagon is rotated by the angle  $2\pi/5$  clockwise.

Similarly, the compositions of two reflections corresponding to the other three diagrams of Figure 2 lead to rotations of the pentagon, respectively, by  $4\pi/5$  counterclockwise, by  $4\pi/5$  clockwise, and by  $2\pi/5$  counterclockwise. If we apply these four transformations, respectively,  $c, d, e,$  and  $f$  times, then the total (clockwise) rotation will be  $2((c - f) + 2(e - d))\pi/5$ . If the latter is not a multiple of  $2\pi$ , we need to traverse the double pentagon (or interval exchange) periodic orbit 5 times to obtain a closed billiard trajectory in the regular pentagon.  $\square$

**Corollary 12** *The ratio of the lengths of the long and short closed billiard trajectories of the same directions is always equal to  $\phi$ .*

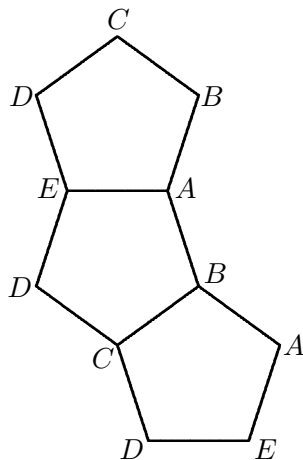


Figure 11: Rotation of the pentagon

**Proof.** One has:  $(C - F) + 2(E - D) = (c + e - d - f) + 2(c - f) = 3(c - f) + (e - d) \equiv 3[(c - f) + 2(e - d)] \pmod{5}$ .  $\square$

**Remark 2.4** A similar fact does not hold for geodesics on a regular dodecahedron: examples show that the ratio between the lengths of parallel geodesics may be different for different directions.

### 3 Proofs

#### 3.1 Double pentagon as a translation surfaces and its Veech group

In this section we briefly review basic facts about translation surfaces (our double pentagon is one) and their symmetries. See [4, 6, 9, 16] for a comprehensive exposition. We specify the general theory to the case of the double pentagon and establish Theorem 1.

A translation surface is a closed surface with conical singularities equipped with an atlas for which the transition functions are parallel translations. For our purposes, we can define a translation surface as a surface that is obtained from a finite collection of plane polygons by identifying pairs of parallel sides by translations.

The group  $SL(2, \mathbb{R})$  acts on plane polygons preserving parallel sides, hence  $SL(2, \mathbb{R})$  acts on the space of translation surfaces. The Veech group  $V_+(X)$  of a translation surface  $X$  consists of those  $g \in SL(2, \mathbb{R})$  for which  $g(X)$  is equivalent to  $X$  as a translation surface. The affine group  $Aff_+(X)$  consists of orientation-preserving homeomorphisms of  $X$  that are affine in local coordinates; the derivative of such an affine diffeomorphism is constant. The group  $V_+(X)$  consists of the derivatives of the transformations in  $Aff_+(X)$ .

Following Smillie and Ulcigrai [10], we extend the above described groups to include orientation reversing transformations:  $Aff(X)$  consists of all affine diffeomorphisms of  $X$ , and  $V(X)$  of their derivatives. Of course, elements of  $Aff(X)$  take periodic trajectories to periodic ones.

A translation surface  $X$  is called a Veech surface if  $V_+(X)$  is a lattice in  $SL(2, \mathbb{R})$  (a discrete finite co-volume subgroup). For Veech surfaces, the dynamical dichotomy described in the Section 1 holds.

In [13], Veech described the group  $V(X)$  for the double pentagon  $X$  and proved that it is a Veech surface. This description is crucial for our purposes.

First of all, symmetries of the regular pentagon provide elements of the group  $Aff(X)$ . Consider the decomposition of the double pentagon into two horizontal strips in Figure 4. Choose the direction of the strips as horizontal, and consider the horizontal Dehn twist, a shear map of both strips (a shear map is given by the formula  $(x, y) \mapsto (x + cy, y)$ ) that leaves the horizontal boundaries intact and wraps vertical segments around the strips once. If the side of the pentagon is unit then  $c = 2 \cot(\pi/5)$ . Borrowing from [10], post-compose the horizontal Dehn twist with reflection in the vertical line; we obtain an affine automorphism  $\Phi \in Aff(X)$ . The derivative of  $\Phi$  is

$$R = \begin{pmatrix} -1 & -2 \cot\left(\frac{\pi}{5}\right) \\ 0 & 1 \end{pmatrix}$$

Note that  $R$  is an involution, and that  $R$  fixes the boundary directions of sector 3 in Figure 5. Note also that  $R$  takes the union of sectors 1, 2, 4, 5 to sector 3.

The group  $V(X)$  is generated by  $R$  and the group of symmetries of the regular pentagon  $D_5$ . We think of elements of the group  $V(X)$  as isometries of the hyperbolic plane. Then  $R$  is a reflection in the vertical side of the regular ideal pentagon in Figure 5, and  $V(X)$  is generated by reflections in the sides of the hyperbolic triangle with angles  $(\pi/2, \pi/5, 0)$ .

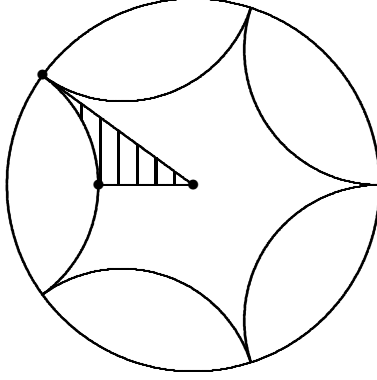


Figure 12:  $(\pi/2, \pi/5, 0)$  triangle

The directions of periodic linear trajectories on  $X$  correspond to the cusps of this group. This set of periodic directions is the set of vertices of the tiling of the hyperbolic plane by ideal pentagons, obtained from the one in Figure 5 by reflections in the sides (the vertices of this ideal pentagon of generation 0 represent the periodic directions parallel to the sides of the double pentagon).

Thus all periodic directions in sector 3 are obtained by an iterative procedure: apply the rotations  $T^m$ ,  $m = 1, 2, 3, 4$ , to a periodic direction of generation  $k$  to obtain a periodic direction in one of the four other sectors, and then apply the reflection  $R$  to take this point to a periodic direction in sector 3 of the next generation  $k + 1$ . This is the mechanism described in Theorem 1 (i). Since  $T$  and  $R$  correspond to affine automorphisms of the double pentagon, they preserve the decomposition into two periodic strips in the periodic direction (statement (ii)). The formulas in statement (iii) are verified directly by induction on  $k$ .

Concerning the last statement of Theorem 1, it is clear that the set of vertices of the tiling by regular ideal pentagons is a subset of  $\mathbb{Q}[\phi] \cup \{\infty\}$ . The non-trivial fact that this set coincides with  $\mathbb{Q}[\phi] \cup \{\infty\}$  follows from the work of A. Leutbecher [5], where this fact is proved for the set of cusp points of the Hecke group  $G(2 \cos(\pi/5))$ , the subgroup of  $SL(2, \mathbb{R})$  generated by the transformations  $z \mapsto -1/z$ ,  $z \mapsto z + 2 \cos(\pi/5)$ . One can also deduce this statement from a description of periodic directions for genus 2 translation surfaces with one conical singularity recently obtained by K. Calta [1] and by C. McMullen [7].

### 3.2 Generating symbolic orbits

Following [10], we consider the pairs of consecutive symbols that may appear in the symbolic orbits in the double pentagon. We present the result in the form of a graph whose vertices correspond to the labels of the sides; an oriented edge from vertex  $i$  to vertex  $j$  means that the pair  $ij$  appears in some symbolic orbit. The answers depend on the sector under consideration. The next lemma is straightforward.

**Lemma 3.1** *The graphs describing pair of consecutive symbols in sectors 1, 2, 3, 4, 5, respectively, are depicted in Figure 13.*

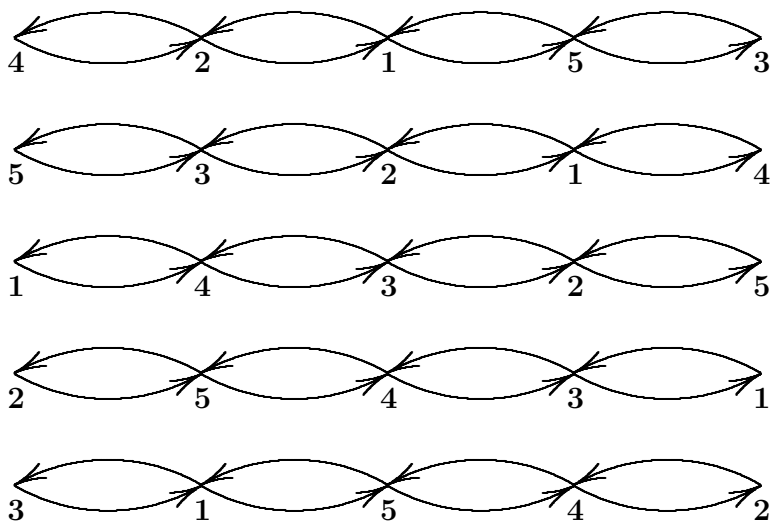


Figure 13: Pairs of consecutive symbols in symbolic orbits

Thus a periodic symbolic trajectory in  $i$ th sector is a periodic path on  $i$ th graph in Figure 13.

Next we examine the effect of the affine map  $\Phi$  on symbolic orbits in sectors 1, 2, 4, 5; the results are symbolic orbits in sector 3. We present the result via enhanced graphs with additional symbols written on the edges, see Figure 14. For a symbolic orbit in sector  $i$ , presented as a periodic path on  $i$ th graph, one traverses this path, inserting the words written on the edges each time the respective edge is passed. We call this the *enhancement* of a symbolic orbit.

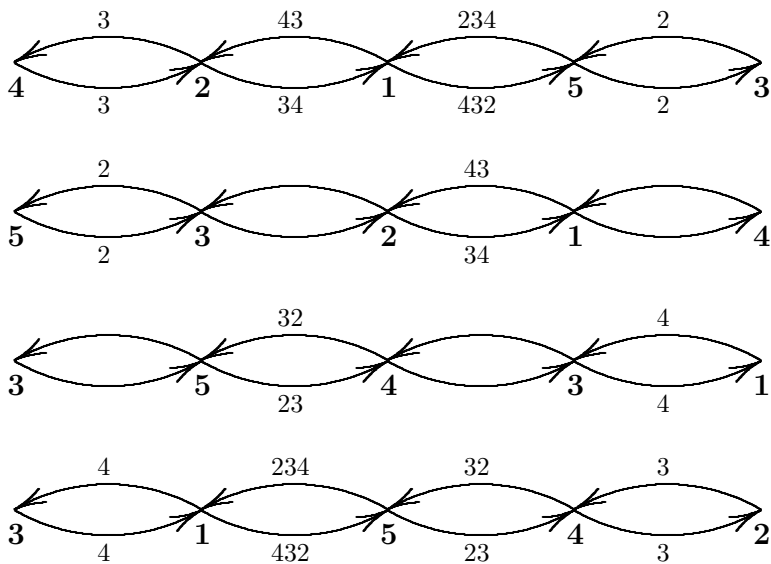


Figure 14: Enhanced graphs

**Lemma 3.2** *Let  $w$  be a symbolic orbit of a periodic trajectory in sector  $i$ . Apply the affine automorphism  $\Phi$  to this trajectory and let  $w'$  be its symbolic orbit (which is a periodic path on 3rd graph in Figure 13). Then  $w'$  is the enhancement of  $w$ .*

**Proof.** We consider the case of 1st sector; the other ones are similar.

Draw the horizontal diagonal in both copies of the pentagon that make the double pentagon and label this diagonal  $e$ , see Figure 15. We add the symbol  $e$  to our alphabet, so the symbolic trajectories will be periodic words in  $\{1, 2, 3, 4, 5, e\}$ . Every trajectory in sector 1 intersects a diagonal marked  $e$  between every two consecutive intersections with the sides. That is, we insert  $e$  between every two symbols 1, 2, 3, 4, 5, which amount to writing  $e$  on each oriented edge of 1st graph in Figure 13.

The shear map affects each segment of a trajectory between the horizontal sides of the two strips into which the double pentagon is split: such a segment is modified by adding one turn around the strip. Symbolically, this is described by the transformations:

$$e3e \mapsto e4e, e4e \mapsto e434e, e2e \mapsto e5e, e5e \mapsto e525e, 1e \mapsto 134e, e1 \mapsto e431.$$

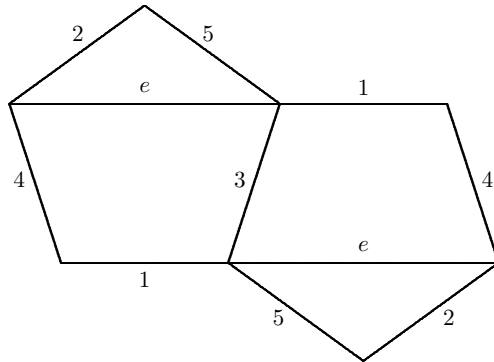


Figure 15: Added diagonal

A reflection in the vertical line is, symbolically, the involution

$$2 \leftrightarrow 5, 3 \leftrightarrow 4, 1 \leftrightarrow 1,$$

so the symbolic action of  $\Phi$  is as follows:

$$e3e \mapsto e3e, e4e \mapsto e343e, e2e \mapsto e2e, e5e \mapsto e252e, 1e \mapsto 143e, e1 \mapsto e341.$$

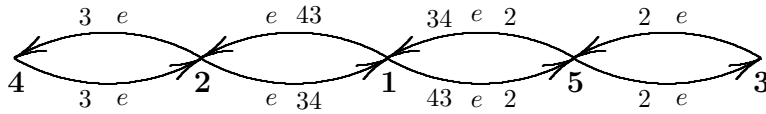


Figure 16: Enhanced 1st graph

This is achieved by enhancement of the graph as shown in Figure 16. It remains to erase the label  $e$ , and we obtain the 1st enhanced graph in Figure 14.  $\square$

We now observe that all four enhanced graphs in Figure 14 are obtained from the graph in Figure 9 as described in Section 2.3.

Let us summarize: given a symbolic periodic orbit in sector 3, apply cyclic shifts to obtain a symbolic trajectories in sectors 1,2,4,5, and enhance these symbolic trajectories by traversing them on the graph in Figure 9. This results in symbolic trajectories in sector 3 of the next generation. This is the generation process described in Theorem 5.

We also deduce Theorem 6. Observe that the sandwiching property holds for all four enhanced graphs in Figure 14: the reduction of an enhanced symbolic orbit is the original orbit.

For example, consider the path in the 1st graph in Figure 14 that visits the vertices  $\dots 3 5 1 2 4 \dots$ . Its enhancement is

$$\dots 2 \mathbf{3} 2 \mathbf{5} 2 3 4 \mathbf{1} 4 3 \mathbf{2} 3 4 \mathbf{3} \dots$$

and the reduction is again  $\dots 3 5 1 2 4 \dots$ .

### 3.3 Further proofs

A symbolic periodic trajectory in sector 3 is a periodic path on graph in Figure 9. Assign to such a path the vector  $(c, d, e, f)$  whose components are the number of times per period that the edges 43, 41, 25, 23 were traversed (in either direction). Thus two such vectors are assigned to every periodic direction; the symbolic period is the sum of the components. For example, the respective pairs of vectors for the first five periodic directions

$$1 - \frac{\phi}{2}, \frac{5\phi - 8}{2}, 0, \frac{8 - 5\phi}{2}, \frac{\phi}{2} - 1$$

in Figure 6 are:

$$\begin{aligned} (0 \ 0 \ 1 \ 0), & \quad (1 \ 0 \ 0 \ 0) \\ (1 \ 1 \ 0 \ 0), & \quad (1 \ 0 \ 1 \ 1) \\ (1 \ 0 \ 0 \ 1), & \quad (1 \ 1 \ 1 \ 1) \\ (0 \ 0 \ 1 \ 1), & \quad (1 \ 1 \ 0 \ 1) \\ (0 \ 1 \ 0 \ 0), & \quad (0 \ 0 \ 0 \ 1). \end{aligned}$$

Note that if  $(a, A)$  and  $(b, B)$  are the first and the last pairs of these vectors, then the three pairs in-between are

$$(b + A, a + A + B), (A + B, a + b + A + B), (a + B, b + A + B). \quad (2)$$

Theorem 5, or the enhanced graphs in Figure 14, tell us how the 4-component vector changes under the generation process: the cyclic shift by  $i \in \{1, 2, 3, 4\}$  and enhancement. In each case, the result is a linear transformation, depending on  $i$ . These transformations, denoted by  $L_i$ , are as follows:

$$L_1(c, d, e, f) = (c+e+f, e, c+d, c), L_2(c, d, e, f) = (c+d+e+f, c+d, c+f, c+e+f),$$

$$L_3(c, d, e, f) = (c+d+f, c+f, e+f, c+d+e+f), L_4(c, d, e, f) = (f, e+f, d, c+d+f).$$

It follows that the linear relation (2) is inherited by the consecutive quintuples of pairs of vectors of each next generation. Applying the linear function

$$p(c, d, e, f) = c + d + e + f$$

to relation (2), we obtain the same relation for periods, that is, the statement of Theorem 2.

Theorem 4 is a reformulation of Theorem 2, as explained in the paragraph that precedes its formulation in Section 2.2; we do not dwell on its proof.

We can deduce Theorem 7 from relation (2). The statement of Theorem 7 is that the 4-component vectors  $(a, A)$  corresponding to a periodic direction satisfy the linear relation  $A = M(a)$  where

$$M = \begin{pmatrix} 1 & 0 & 1 & 0 \\ 0 & 0 & 0 & 1 \\ 1 & 0 & 0 & 0 \\ 0 & 1 & 0 & 1 \end{pmatrix}.$$

Note that  $M^2 = M + I$ .

Assuming that  $A = M(a), B = M(b)$ , we want to deduce the same relations for the vectors in (2). Indeed,

$$a + A + B = a + M(a) + M(b) = M^2(a) + M(b) = M(A + b),$$

$$a + b + A + B = a + b + M(a) + M(b) = M^2(a) + M^2(b) = M(A + B),$$

$$b + A + B = b + M(a) + M(b) = M(a) + M^2(b) = M(a + B),$$

and Theorem 7 follows.

Let us also prove Theorem 10. The components of the vector  $(c, d, e, f)$  are the numbers of symbols I, II, III, IV in a periodic symbolic orbit. When the respective periodic trajectory is unfolded in the plane, each symbol III = 25 corresponds to the vector  $u$ , the symbol I = 43 to the vector  $\phi u$ , the symbol II = 41 to the vector  $v$ , and the symbol IV = 23 to the vector  $\phi v$ , see Figure 17. The displacement vector is then  $(c\phi + e)v + (f\phi + d)u$ , as claimed.

For a regular pentagon with the side length 1, the distance from a vertex to the nearest diagonal not passing through this vertex equals  $\sin 36^\circ$ ; the distance between a side and the diagonal parallel to this side equals  $\sin 72^\circ = \phi \sin 36^\circ$ . Hence, the displacement corresponding to symbols II

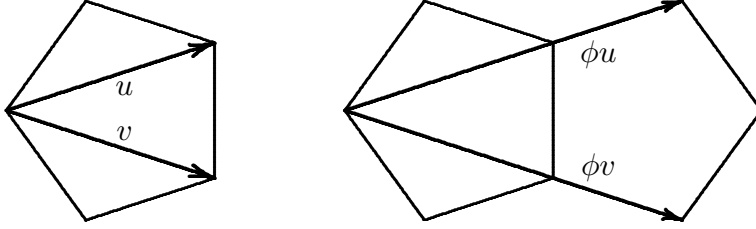


Figure 17: Displacement vectors

and III, measured in the directions of the bisector between  $u$  and  $v$  equals  $(1 + \phi) \sin 36^\circ = \phi^2 \sin 36^\circ$ , and the displacement, corresponding to the symbols I and IV, measured in the same direction, is  $(1 + 2\phi) \sin 36^\circ = \phi^3 \sin 36^\circ$ . The full displacement is  $((c + f)\phi^3 + (d + e)\phi^2) \sin 36^\circ$ . To find the length of the actual orbit, we need to divide the result by the cosine of the angle between the direction and the bisector, and we obtain the formula stated in Theorem 10.

The two displacement vectors are obtained from the ones, corresponding to the simplest periodic orbits (in the direction  $u$ ), by a linear transformation. The displacement vectors for the latter are  $u$  and  $\phi u$ . It follows that the two vectors are also proportional with coefficient  $\phi$ :

$$(C\phi + E)v + (F\phi + D)u = \phi((c\phi + e)v + (f\phi + d)u).$$

This again implies the relations of Theorem 7.

## 4 Expected further results

Results similar to the ones of these paper may hold for billiards in all regular polygons and linear flows on double odd-gons or regular even-gons (in both cases, the parallel sides are identified by translations). As we mentioned earlier, the case of regular octagon was studied recently by J. Smillie and C. Ulcigrai ([10, 11]). In addition to the results of these works, we can provide a description of periods of periodic orbits.

A billiard trajectory in a regular octagon is closed if the slope of the trajectory belongs to  $\mathbb{Q}[\sqrt{2}]$  (we assume that some side is horizontal). These directions can be arranged on the projective line – the absolute of the hyperbolic plane – in the following way. First we consider an ideal regular octagon; its vertices, in Figure 18, are marked by the slopes.

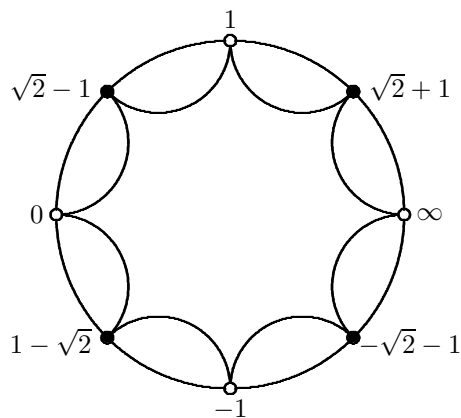


Figure 18: Directions of periodic geodesics for an octagon

As it is seen in Figure 18, the vertices are marked, alternatively, black and white. Then we construct the first generation of octagons by reflection in the sides of the big octagon, then the next generation, and so on. For example, the vertices of the octagon of the first generation between the points  $\sqrt{2} - 1$  and 0 are

$$\sqrt{2} - 1, \frac{2\sqrt{2} - 1}{7}, \frac{3 - \sqrt{2}}{7}, \frac{\sqrt{2} - 1}{2}, \frac{3\sqrt{2} - 1}{17}, 3 - 2\sqrt{2}, \frac{\sqrt{2} - 1}{3}, 0,$$

and the vertices of the octagon of the second generation between  $\sqrt{2} - 1$  and  $\frac{2\sqrt{2} - 1}{7}$  are

$$\sqrt{2} - 1, \frac{3\sqrt{2} - 2}{7}, \frac{3\sqrt{2} + 1}{17}, \frac{10\sqrt{2} - 9}{17}, \frac{15\sqrt{2} - 9}{41}, \frac{1 - \sqrt{2}}{2}, \frac{11\sqrt{2} - 9}{23}, \frac{2\sqrt{2} - 1}{7}.$$

All vertices of all octagons are marked, alternatively, by white or black dots, and the reflections, as well as rotations by  $90^\circ$ , preserve these marking.

For each of these points, there are two periods. For example, for  $\sqrt{2} - 1$ , the periods are 1 and 2; for 0, the periods are 2 and 2. A theorem similar to Theorem 2 states that for the eight vertices of any generation, the pairs of periods look as in Figure 19 (one can flip it upside down).<sup>2</sup>

There also holds a statement similar to Theorem 3, but the difference of the arithmetic sequence depends on the marking of the point  $\beta$ : if  $\beta$  is

<sup>2</sup>J. Smillie gave a proof of this result after we informed him about it.

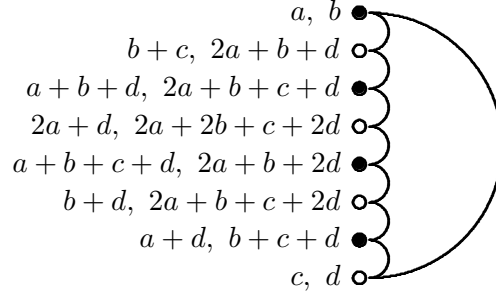


Figure 19: Periods in the octagon

a white dot, then the difference is  $(B, b + B)$ , but if it is black, then the difference is  $(B, 2b + B)$ . All other results of Section 2 also have their analogs for octagon.

The results are different for regular heptagons. For those, we have a sequence of generations of ideal regular heptagons, and for every vertex of every heptagon there are three periods (this 3 is the genus of a flat surface obtained from the double heptagon). If for a heptagon of some generation the triples of periods corresponding to two vertices joined by an arc are  $(a_1, a_2, a_3)$ ,  $a_1 \leq a_2 \leq a_3$  and  $(b_1, b_2, b_3)$ ,  $b_1 \leq b_2 \leq b_3$ , then the periods at the five intermediate vertices are:

- $a_1, a_2, a_3$
- $a_2 + b_1, a_1 + b_2 + a_3, a_2 + b_3 + a_3$
- $a_3 + b_2, a_2 + a_3 + b_1 + b_3, a_1 + a_2 + a_3 + b_2 + b_3$
- $a_3 + b_3, a_2 + a_3 + b_2 + b_3, a_1 + a_2 + a_3 + b_1 + b_2 + b_3$
- $a_2 + b_3, a_1 + a_3 + b_2 + b_3, a_2 + a_3 + b_1 + b_2 + b_3$
- $a_1 + b_2, a_2 + b_1 + b_3, a_3 + b_2 + b_3$
- $b_1, b_2, b_3$

A statement similar to Theorem 3 in the case of a regular heptagon looks very simple. If the triple of periods for a point  $\beta$  is  $(a, b, c)$ , then the triples of periods of points  $\gamma_i$  (with an appropriate sign change) form an arithmetic sequence with the difference  $(b, a + c, b + c)$ .

We conjecture that similar results hold, at least, for all regular polygons.

## References

- [1] K. Calta. *Veech surfaces and complete periodicity in genus two*. J. Amer. Math. Soc. 17 (2004), 871–908.
- [2] D. Fuchs. *Geodesics on a regular dodecahedron*. Preprint, MPIM 2009.
- [3] D. Fuchs, E. Fuchs. *Closed geodesics on regular polyhedra*. Mosc. Math. J. 7 (2007), 265–279.
- [4] P. Hubert, T. Schmidt. *An introduction to Veech surfaces*. Handbook of dynamical systems. Vol. 1B, 501–526, Elsevier, Amsterdam, 2006.
- [5] A. Leutbecher. *Über die Heckschen Gruppen  $G(\lambda)$* . Abh. Math. Sem. Univ. Hamburg 31 (1967), 199–205.
- [6] H. Masur, S. Tabachnikov. *Rational billiards and flat structures*. Handbook of dynamical systems, Vol. 1A, 1015–1089, North-Holland, Amsterdam, 2002.
- [7] C. McMullen. *Billiards and Teichmüller curves on Hilbert modular surfaces*. J. Amer. Math. Soc. 16 (2003), 857–885.
- [8] D. Rosen. *A class of continued fractions associated with certain properly discontinuous groups*. Duke Math. J. 21, (1954). 549–563.
- [9] J. Smillie. *The dynamics of billiard flows in rational polygons*. Dynamical systems, ergodic theory and applications. 2nd edition. Encycl. Math. Sciences, 100. Springer, Berlin, 2000.
- [10] J. Smillie, C. Ulcigrai. *Symbolic coding for linear trajectories in the regular octagon*. Preprint arXiv:0905.0871.
- [11] J. Smillie, C. Ulcigrai. *Geodesic flow on the Teichmüller disk of the regular octagon, cutting sequences and octagon continued fractions maps*. Preprint arXiv:1004.2265.
- [12] S. Tabachnikov. *Billiards*. Panor. Synth. No. 1 (1995).
- [13] W. Veech. *Teichmüller curves in moduli space, Eisenstein series and an application to triangular billiards*. Invent. Math. 97 (1989), 553–583.

- [14] W. Veech. *The billiard in a regular polygon*. *Geom. Funct. Anal.* 2 (1992), 341–379.
- [15] Ya. Vorobets. *Plane structures and billiards in rational polygons: the Veech alternative*. *Russian Math. Surveys* 51 (1996), 779–817.
- [16] A. Zorich. *Flat surfaces*. *Frontiers in number theory, physics, and geometry. I*, 437–583, Springer, Berlin, 2006.